Ultrastructural Changes and Structure and Mobility of Myowater in Frozen-Stored Hake (*Merluccius merluccius* L.) Muscle: Relationship with Functionality and Texture

A. M. HERRERO,[†] P. CARMONA,[‡] M. L. GARCÍA,[§] M. T. SOLAS,[#] AND M. CARECHE*,[†]

Instituto del Frío, CSIC, Jose Antonio Novais, 10 Ciudad Universitaria, 28040 Madrid, Spain;
Instituto de Estructura de la Materia, CSIC, Serrano, 121, 28006 Madrid, Spain; Centro de
Microscopia Electrónica Luis Bru, Universidad Complutense de Madrid, 28040 Madrid, Spain;
Departamento de Biología Celular, Facultad de Ciencias Biológicas,
Universidad Complutense de Madrid, 28040 Madrid, Spain

The ultrastructural changes and the main Raman spectral features of water (3100−3500 and 50−600 cm^{-1} ranges) in frozen-stored hake were studied with the aim of connecting these changes with loss of some functional properties such as water holding capacity, and with modifications of muscle texture. The following results were obtained: (a) The changes in the spaces between myofibrils can be related to modifications of shear resistance. (b) The behavior of the strong 160 cm^{-1} band can be related to conformational transitions of muscle proteins, to changes in the structure of muscle water, and/or to alterations in protein−water interactions. (c) There were intensity changes in the ν_s(OH) band that may be attributable to transfer of water to larger spatial domains during frozen storage.

KEYWORDS: Fish muscle water; Raman spectroscopy; ultrastructure; WHC; texture

INTRODUCTION

During the freezing process, and especially during frozen storage, fish muscle can undergo a number of changes that determine the storage life of frozen seafoods. Most studies on changes in frozen-stored fish have focused on the alteration of myofibrillar proteins because of their role as determinants of functionality and texture. It has long been recognized that denaturation and aggregation during prolonged frozen storage are accompanied by loss of functional properties such as water holding capacity, extractability, or apparent viscosity, as well as toughening of fish muscle. Structural changes have been observed in proteins during frozen storage, including loss of the α-helical proportion at the expense of β-sheets and increased exposure of hydrophobic aliphatic side chains (*1, 2*). However, some of these structural changes are not directly related to modifications observed in fish muscle texture or functionality.

The ultrastructure of fish muscle is also affected during frozen storage. Changes include (a) modifications of the morphology of fibers due to ice crystal formation (*3−6*), (b) reduction of the sarcoplasmic space between myofibrils (*4−8*), and (c) reduction of interfilament distance (*8−10*).

Structural changes in proteins and ultrastructural alterations of fish muscle may be accompanied by changes in the association between protein and water molecules and in the distribution and mobility of the water in the tissue. Low-field nuclear magnetic resonance (NMR) spectroscopy has shown that there are several domains or pools of water which are characterized by their water proton relaxation time. Changes in these water proton relaxation times have been observed during frozen storage, varying consistently with frozen storage conditions (*11−13*). Raman spectroscopy has proven to be a powerful tool for investigating the structure of water in solutions of biological macromolecules and complex biological systems, including muscle fibers (*14−19*). The main spectral features of the Raman spectrum of water in fish muscle can be summarized as follows: (i) the broad band between 3100 and 3500 cm^{-1}, which is attributable to OH stretching motions, and (ii) the low-frequency range (below 600 cm^{-1}), which is related to intermolecular water and protein librations and restricted translational motions involving the bending and stretching vibrations of the O(N)−H···O(N) units. This spectral range below 600 cm^{-1} shows intermolecular fluctuation bands which are due to interactions of hydrogen-bonded water and biomolecules (*17, 20*).

We present here the ultrastructural changes and the spectral behavior of the above Raman regions in fish muscle in the course of frozen storage, and their relationship with the functional properties and texture, in frozen storage conditions rendering very different practical storage times (−10 and −30 °C). The aim is to gain some understanding of the causes of the detrimental changes occurring in frozen-stored fish.

* To whom correspondence should be addressed. Phone: 34 91 5492300. Fax: 34 91 5493627. E-mail: mcareche@if.csic.es.
[†] Instituto del Frío.
[‡] Instituto de Estructura de la Materia.
[§] Centro de Microscopia Electrónica Luis Bru.
[#] Departamento de Biología Celular.

Structural Changes in Hake Muscle during Frozen Storage

J. Agric. Food Chem., Vol. 53, No. 7, 2005 **2559**

MATERIALS AND METHODS

Fish Source. Gutted hake (*Merluccius merluccius* L.) were obtained from the Galician shelf. The average length and mass of the fish were 51.4 ± 2.4 cm and 1300 ± 250 g, respectively. The fish were transported in ice to the Instituto del Frío (CSIC) in insulated containers with a perforated platform inside to prevent contact between the fish and melted ice. The fish, in *postrigor* condition, were headed, filleted, and washed with iced water to remove blood and the remains of viscera. Some fillets were analyzed unfrozen, and the rest were frozen in a blast freezer (Frigoscandia, Aga Frigoscandia, Freezer Division, Helsingborg, Sweden) until the center reached −40 °C (within 1.30 h), vacuum packed in Cryobac BB-1 bags, and stored at −10 and −30 °C until analysis. Frozen fillets were thawed (4 °C overnight) for each temperature and storage time. Fillets from three individuals were used in each sampling day. Analyses were performed unfrozen (0), and at 1, 7, 16, 24, and 38 weeks.

Water Holding Capacity (WHC). A 2 g sample covered by filter paper was centrifuged at 1500 rpm for 5 min. Results were expressed as grams of water retained in the sample per 100 g of water present in the sample before centrifugation (%) (*21, 22*). Measurements were made at least in triplicate.

Textural Analysis. Determinations were performed using an Instron model 4501 universal testing machine (Instron Corp., Canton, MA) and Instron Series IX software (Automated Materials Testing System V.5). A Kramer shear resistance test was carried out (*23*) with a head which exerted a maximum force of 5 kN at a speed of 100 mm/min. Maximum force was measured in newtons per gram. A minimum of six replicates were performed per assay (*24*).

Transmission Electron Microscopy. Pieces of 3×2 cm were removed from the fillets after thawing. The pieces were immediately fixed in 2.5% glutaraldehyde in 0.1 M phosphate buffer, pH 7.2, postfixed in 1% osmium tetroxide, dehydrated in a graded series of acetone, and finally embedded in Epon. Thin sections were obtained transversally to the muscle fibers and stained with 2% uranyl acetate followed by lead citrate. Electron micrographs were examined with a model 902 electron microscope (Carl Zeiss, Oberkochen, Germany) with a Canstaing-Henry-Ottensmeyer energy filter.

Raman Spectroscopy. Small portions from different parts of hake fillets were transferred to glass tubes (5 cm height and 5 mm i.d.; Wilmad Glass Co., Inc., Buena, NJ) to fill ∼1 cm length (*1*). The tube containing the sample was sealed and placed in a thermostated device at 15−20 °C for Raman analysis. Raman spectra were obtained using a Bruker RFS 100/S FT spectrometer equipped with a notch filter and a liquid nitrogen-cooled germanium detector. The excitation source was a Nd:YAG laser operating at a wavelength of 1064 nm with about 300 mW of power. The scattered radiation was collected at 180° to the source, and frequency-dependent scattering of the Raman spectra measured with this spectrometer was corrected by multiplying point by point with $(\nu_{laser}/\nu)^4$. Spectra were recorded at 4 cm^{-1} resolution, and the reported Raman frequencies from signal-averaged spectra are accurate to ±0.5 cm^{-1}. Measurements were performed in three fillets. Three portions were analyzed per fillet, and 2000 scans were recorded for each sample, resulting in a total of 6000 scans per fillet. Raman spectra were compared and evaluated using SpectraCalc (Galactic Industries, Salem, NH) and Opus 2.2 (Bruker, Karlsruhe, Germany) software.

The vibrational modes were assigned according to the literature (*15, 17, 25−28*). Due to the necessity of using a filter to cut away the intensity Rayleigh line, including the most intense part of the Rayleigh wing, the low-frequency region may seem difficult to investigate. However, with recent FT-Raman technology there are filters available which allow investigation down to frequencies as low as 50 cm^{-1} (*20*). In addition, the high intensity of the Rayleigh line can be removed by $R(\nu)$ representation (*20*), so that the Rayleigh line is converted into a plateau:

$$R(\nu) = \nu[1 - \exp(-hc\nu/kT)]\,I(\nu)$$

where $I(\nu)$ is the intensity in the Raman spectrum at a frequency of ν cm^{-1}, c is the speed of light, T is the absolute temperature, and h and k are Planck's and Boltzmann's constants, respectively.
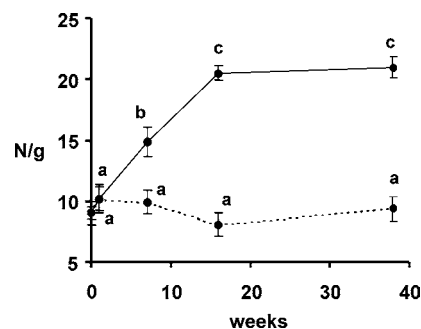

Figure 1. Shear resistance values (N/g) measured by Kramer shear compression from hake muscle: fresh muscle stored at −10 °C (solid lines) and −30 °C (dotted lines) (mean ± SEM). Different letters for the same temperature indicate significant differences ($P < 0.05$).
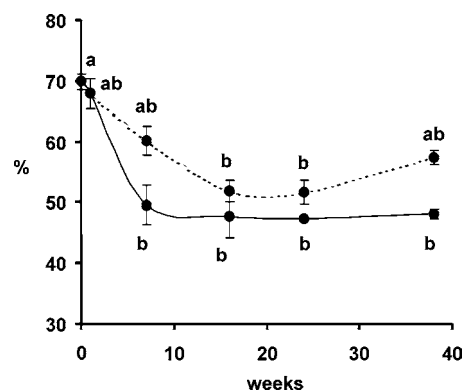

Figure 2. Water holding capacity (%) from fresh hake fillets fresh-stored at −10 °C (solid lines) and −30 °C (dotted lines) (mean ± SEM). Different letters for the same temperature indicate significant differences ($P < 0.05$).

The intensity of the Raman band near 1450 cm^{-1} due to methylene and methyl bending modes has been reported to be insensitive to the microenvironment and was therefore used as an internal standard for normalization of the spectra (*2, 29−32*).

Statistical Analyses. Analysis of variance (ANOVA) was performed with storage time as covariate, to see the effect of storage temperature (−10 and −30 °C). Then, one-way analysis of variance was performed for each temperature, with storage time as the factor. The Levene test was used to check the equality of variances. Where variances were equal, the difference between means was analyzed by the F test. Where equality of variances could not be assumed, Welch & Brown-Forsythe's robust test for equality of means was used. Once the difference between means was assumed, multiple paired comparisons were used to determine which means differed from one another. The Bonferroni test was used where variances were presumed equal, and the Tamhane T2 test was used where equality of variances could not be assumed. The software used was SPSS 11.5 (SPSS Inc., Chicago, IL).

RESULTS

Shear Resistance and Water Holding Capacity. **Figures 1** and **2** show, respectively, the Kramer shear resistance values and the WHC of frozen-stored hake muscle, and **Table 1** shows their analysis of variance. Kramer shear resistance increased significantly only in samples stored at −10 °C. As expected, −30 °C stored samples did not present significant variations in this parameter (*1*).

There were significant changes of WHC with storage time for both temperatures studied. WHC decreased significantly over the first 7 weeks in samples stored at −10 °C and over the first 16 weeks at −30 °C; there were no major differences thereafter.

Electron Microscopy. *Fiber Organization.* The organization of fibers in fresh muscle is shown in **Figure 3A**. Plasmalemma was partially disrupted. Mitochondria and membrane vesicles

2560 *J. Agric. Food Chem.,* Vol. 53, No. 7, 2005

Herrero et al.

Table 1. One-Way Analysis of Variance as a Function of Temperature with Storage Time as Covariate for the Variables Listed Below[a]

variable	model	temperature	storage time
Kramer shear resistance	***	***	*
water holding capacity	***	NS (limit)	**
Raman band at 160 cm^{-1}	***	*	***
Raman band at 440 cm^{-1}	NS	NS	NS
Raman band at 3220 cm^{-1}	NS	NS	*

[a] Significance established at 0.05 (*), 0.01 (**), and 0.001 (***) levels. NS = nonsignificant.

were visible in the subsarcolemmal space. No changes were observed in frozen samples examined after one week in frozen storage.

In samples stored at −10 °C for 24 weeks, no obvious change was observed in the distance of fibers compared to that of the control, except for some areas where extracellular spaces were large due to the presence of ice crystals. Membrane residues, mitochondria remnants, and material resembling aggregated proteins were found between fibers (**Figure 3B**).

At 38 weeks of storage at −10 °C, in some areas fibers seemed more compacted when compared to those of the samples stored at −10 °C for 24 weeks. The area between two adjacent fibers contained compressed membrane, mitochondria remnants, and collagen fibers, as in samples stored for 24 weeks (**Figure 3C**). However, there were abundant voids between fibers, indicating the presence of ice crystals. Many fibers were broken, presenting an irregular shape due to the pressure exerted by extracellular and intracellular ice crystals. The little material found in these areas consisted mainly of ruptured sarcolemma and amorphous material (**Figure 3D**).

The space between fibers did not alter significantly in muscle stored at −30 °C for either 24 or 38 weeks. However, in muscle stored for 38 weeks, interfiber spaces were occasionally enlarged by the presence of intracellular and/or extracellular ice crystals (**Figure 3E**).

Intermyofibrillar Spaces. In fresh muscle and samples frozen-stored for one week, myofibrils were surrounded by the sarcoplasmic reticulum and the transverse tubular (T) system, consisting of a conglomeration of spherical vesicles (**Figure 4A**). Muscle stored at −10 °C for 24 weeks (**Figure 4B**) showed
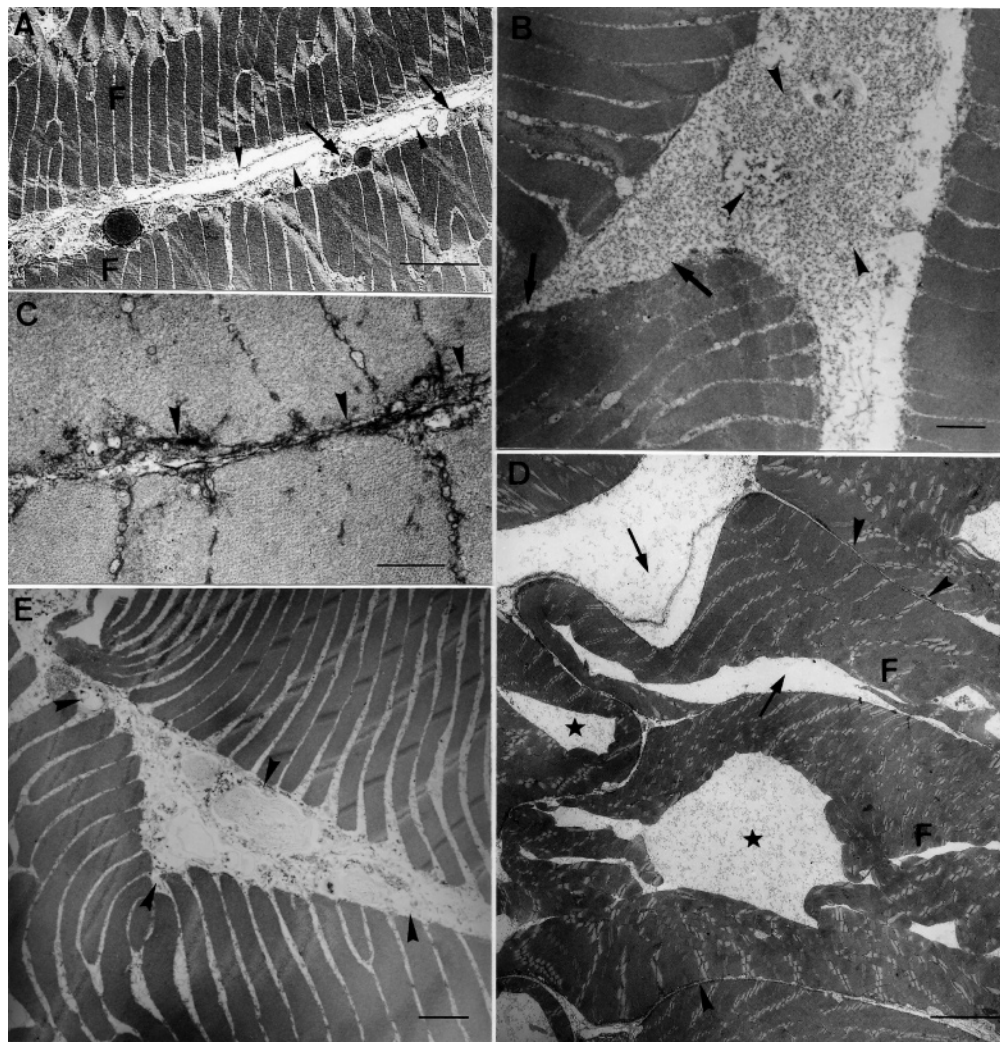

Figure 3. (**A**) Fresh postrigor muscle. Note the disrupted sarcolemma (▼) and the presence of mitochondria (→) in the subsarcolemmal space. Bar = 5.5 μm. (**B**) Hake muscle stored at −10 °C for 24 weeks. Note some wider interfiber spaces in the area occupied by ice crystals (→). Amorphous material, probably denatured proteins, was found (▼). Bar = 1.1 μm. (**C**) Muscle stored at −10 °C for 38 weeks showing a reduction in the space between fibers. Note the compressed membrane remnants between two adjacent fibers (▼). Bar = 0.6 μm. (**D**) Muscle stored at −10 °C for 38 weeks. In some areas fibers are closely packed (▼). Note the local expansion of the space between fibers caused by the presence of ice crystals (→). Intracellular ice crystals are indicated by a star. Bar = 11 μm. (**E**) Muscle stored at −30 °C for 38 weeks. Note the enlargement of the interfiber spaces by the presence of extracellular ice crystals (▼). Bar = 2.5 μm. F = fibers.

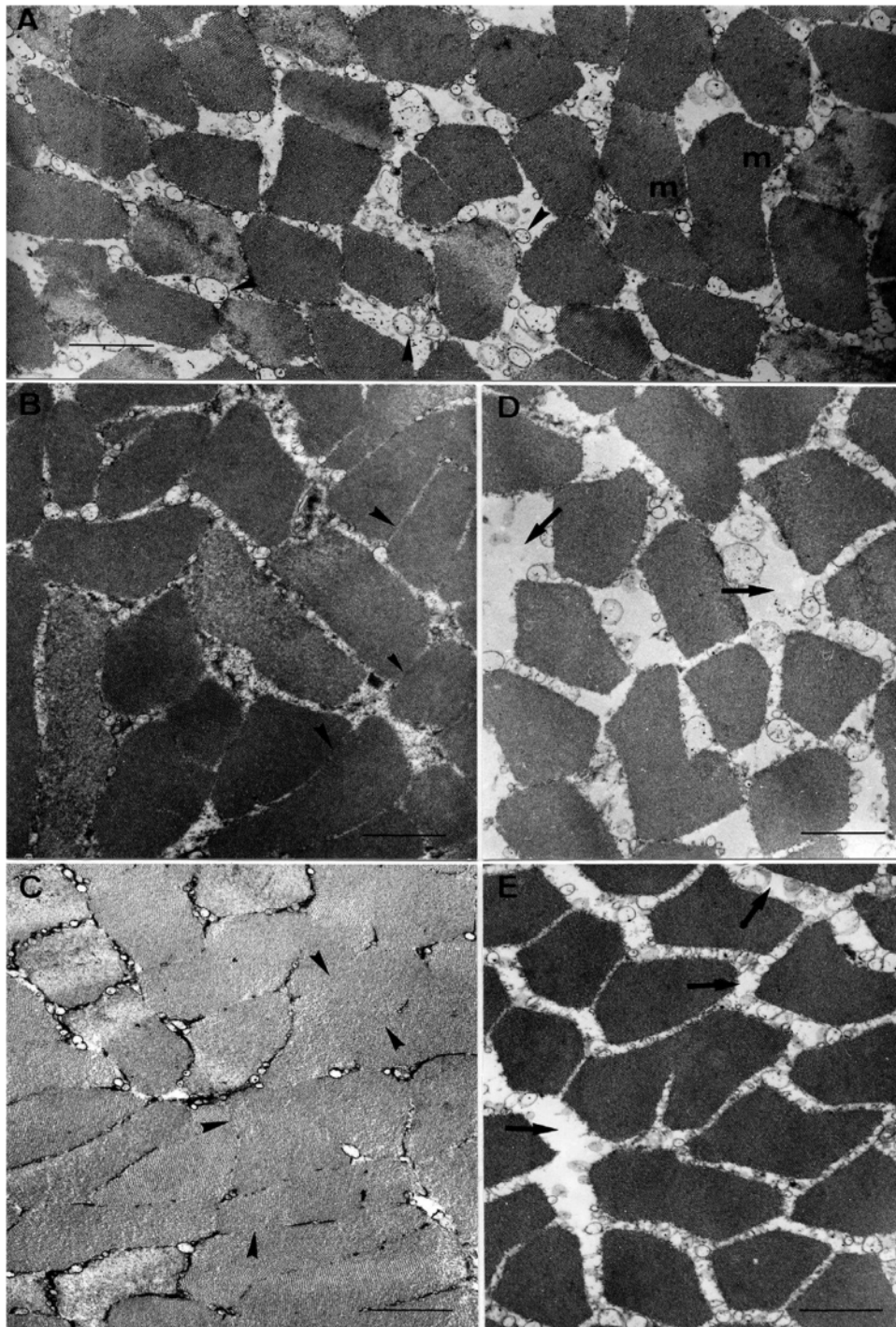**Figure 4.** (**A**) Fresh postrigor muscle. Note the spherical vesicles between myofibrils (▼). m = myofibril. Bar = 1.1 μm. (**B**) Muscle stored at −10 °C for 24 weeks showing a considerable reduction of the space between myofibrils. Note cementation between some myofibrils (▼). Bar = 1.1 μm. (**C**) Muscle stored at −10 °C for 38 weeks. Intermyofibrillar space is dramatically reduced, and myofibrils appear cemented. Note the absence of the sarcoplasmic reticulum in some areas (▼). Bar = 1.1 μm. (**D**, **E**) Muscle stored at −30 °C for 24 and 38 weeks, respectively. Note the regular and wide spaces between myofibrils (→). Bars = 1.1 μm.

a significant reduction of the intermyofibrillar space. There was some cementation of the myofibrils. In samples stored for 38 weeks, the sarcoplasmic reticulum was compressed into a thin layer, and at most locations it became barely visible, so that the myofibrils appeared tightly packed with no space between (**Figure 4C**). There were no observable reductions in the intermyofibrillar space in samples stored at −30 °C for 24 and 38 weeks, which exhibited regular spaces between myofibrils similar to those seen in the control (**Figures 4D,E**).

Filament Lattice. Previous studies have shown that the pattern of thin filaments is disrupted earlier during frozen storage (*33*), and therefore, thick filaments were used to study the alteration of the filament lattice.

Fresh muscle showed the typical hexagonal arrangement of filaments (**Figure 5A**). In samples frozen for one week, most of the fibers retained the regular packing of the filament lattice, but some of them presented myofibrils with reduced interfilament distances and fusions between thick filaments (**Figure**
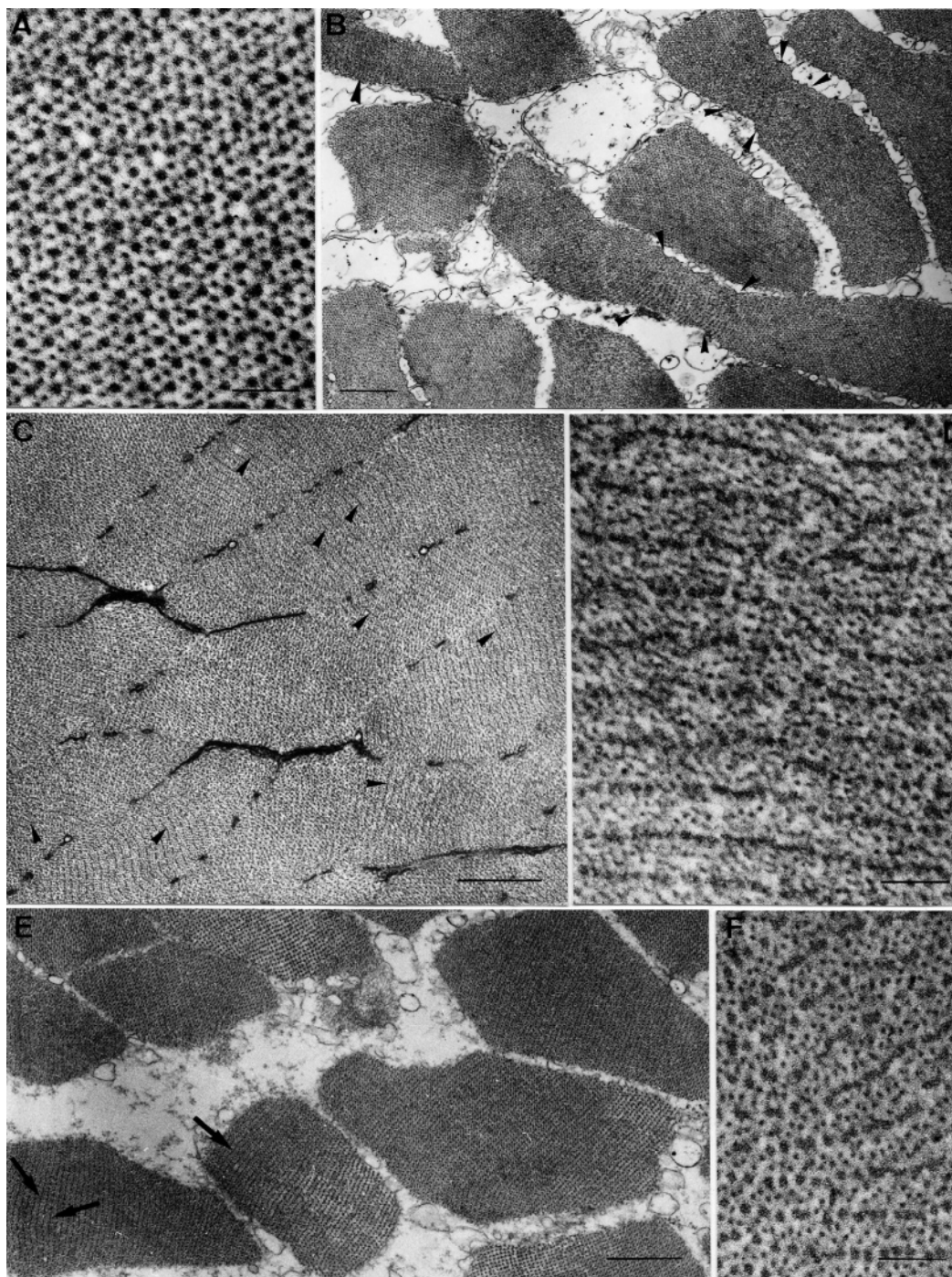
Figure 5. (**A**) Fresh muscle showing the regular hexagonal array of thick filaments. Bar = 75 nm. (**B**) One week frozen sample. Note the reduction of the interfilament distance in some myofibrils (▼). Bar = 0.55 μm. (**C, D**) Muscle stored at −10 °C for 38 weeks. (**C**) Most of the myofibrils present fusions between thick filaments in the 10–10 crystallographic direction (▼). Bar = 0.6 μm. (**D**) Detail at higher magnification of the rows of fused thick filaments. Bar = 75 nm. (**E, F**) Transverse section from muscle stored at −30 °C for 38 weeks. (**E**) Note the presence of myofibrils with reduced interfilament distance (→). Bar = 0.55 μm. (**F**) High magnification of the fused thick filaments. Bar = 75 nm.

5B). The same was found in samples stored at −10 °C for 24 weeks, whereas at 38 weeks of storage at −10 °C, in most of the myofibrils in the whole fibers the spacing between thick filaments in the 10−10 plane was so reduced that they touched, forming rows of fused thick filaments (**Figure 5C,D**). Muscle stored at −30 °C for 24 weeks showed an array of thick filaments similar to that seen in one week frozen-stored samples. In samples stored at −30 °C for 38 weeks, the myofibrils in some fibers retained the regular hexagonal array, but there was an increase in the number of fibers containing abundant

myofibrils in which thick filaments were close together and fused (**Figure 5E,5F**).

Raman Spectroscopy. *Region below 600 cm^{-1}.* **Figure 6** shows the low-frequency range (below 600 cm^{-1}) of the Raman spectrum of hake muscle. A Raman band from water appears near 450 cm^{-1}, which has been attributed to librational or restricted rotation (*17*, *27*). The intensity of this broad band did not change significantly over frozen storage (**Tables 1** and **2**).

The original spectrum of fresh hake muscle exhibits a spectral profile below 200 cm^{-1} with an intensity maximum around 120
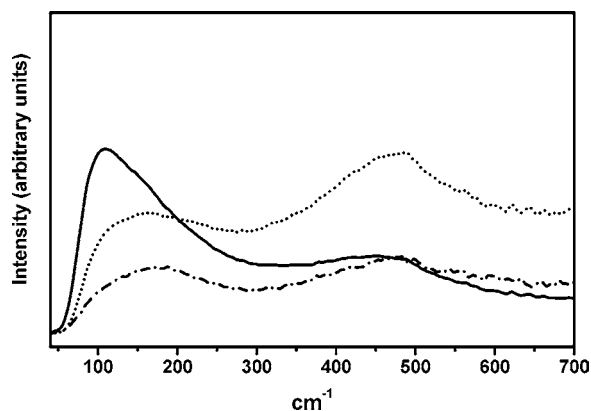
Structural Changes in Hake Muscle during Frozen Storage

J. Agric. Food Chem., Vol. 53, No. 7, 2005 **2563**

Figure 6. Raman spectra in the low-frequency region (below 600 cm^{-1}) of fresh hake muscle: (—) original spectrum; (•••) $R(\nu)$ spectrum of fresh hake muscle; (-••-) $R(\nu)$ spectrum of water.

Table 2. Changes in the Normalized Intensities of the 440 cm^{-1} Water Band from Fresh Hake Muscle Frozen-Stored at −10 and −30 °C[a]

no. of weeks	−30 °C	−10 °C	no. of weeks	−30 °C	−10 °C
0	0.37 ± 0.02	0.37 ± 0.02	16	0.35 ± 0.02	0.34 ± 0.02
1	0.37 ± 0.01	0.37 ± 0.01	24	0.35 ± 0.01	0.35 ± 0.01
7	0.35 ± 0.01	0.32 ± 0.01	38	0.38 ± 0.03	0.38 ± 0.01

[a] Mean ± SEM. Nonsignificant differences were found.

cm^{-1} (**Figure 6**). This relatively strong intensity results from overlapping of water and biomolecule Raman signals and Rayleigh radiation. After removal of the latter by $R(\nu)$ plotting, the resulting spectral profile presents a maximum around 160 cm^{-1}. In contrast, the restricted translational motions of water molecules involved in hydrogen bond interactions are usually observed near 180 cm^{-1} for pure liquid water (*20*), as shown by the $R(\nu)$ spectrum included in **Figure 6**. The 180 cm^{-1} Raman band of bulk water reflects a tetrahedron intermolecular frame and is mainly due to motions of atoms involved in hydrogen bonding (*17, 34*). The frequency downshifting of this band in biological aqueous media has been explained in terms of binding of water molecules to other biomolecules. The $R(\nu)$ spectrum of fish muscle below 200 cm^{-1} (**Figure 6**) can therefore be ascribed to band contributions from the following vibrational modes: (a) motions involving atoms in hydrogen bonding (*20*) such as occur in secondary and tertiary structures through protein−protein and protein−water contacts and other biomolecule−water interactions and (b) translation motions of autoassociated water molecules, as occurs in bulk water. These vibrational modes cannot be resolved because of the small contribution from bulk water and/or the fact that they generate very broad bands, and therefore, the only clear intensity maximum below 200 cm^{-1} is 160 cm^{-1}. The normalized intensity of this band in fish muscle (**Figure 7**) decreases significantly with storage time and temperature (**Table 1**). This effect is more pronounced after about 16 weeks in frozen storage and at −10 °C.

OH Stretching Region. **Figure 8** shows the Raman spectrum of hake muscle in the 3000−3600 cm^{-1} region. The intramolecular vibrations of hydrogen-bonded water include two O−H stretching bands in this region (*17*). The symmetric band (ν_s(OH)) appears around 3220 cm^{-1}, whereas the asymmetric band (ν_{as}(OH)) that normally appears at around 3400 cm^{-1} is not distinctively resolved in our spectra because of a drop in detector sensitivity in this region. Given their N−H stretching
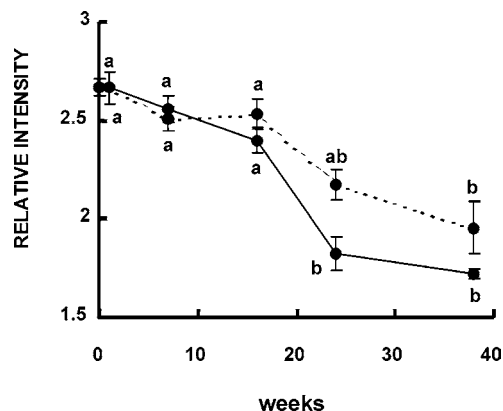

Figure 7. Relative intensity of the 160 cm^{-1} Raman band from fresh hake fillets stored at −10 °C (solid lines) and −30 °C (dotted lines) (mean ± SEM). Different letters for the same temperature indicate significant differences ($P < 0.05$).

Figure 8. Raman spectra in the O−H region (3000–3600 cm^{-1}) of fresh hake muscle.

Figure 9. Relative intensity of the ν(OH) Raman band (3220 cm^{-1}) from fresh hake fillets stored at −10 °C (solid lines) and −30 °C (dotted lines) (mean ± SEM). Different letters for the same temperature indicate significant differences ($P < 0.05$).

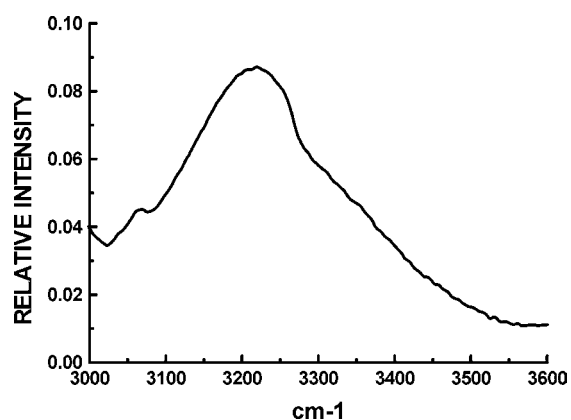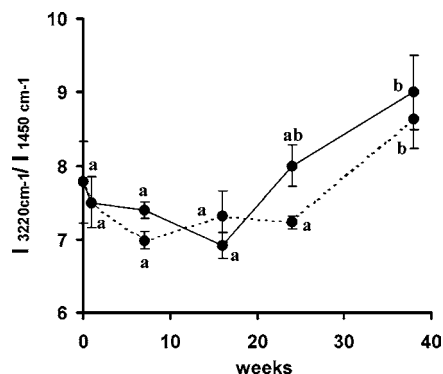vibrational modes, proteins would be expected to contribute to this spectral region, but protein influence on the spectra may be discounted for the following reasons. First, muscle is typically composed of 17% proteins and 80% water, by weight. Second, the particular location of the protein N−H stretching bands is about 3330 cm^{-1}, which is far from the maximum intensity of the spectral profile (**Figure 8**) and falls within a spectral range where the detector sensitivity is much lower than at the 3220 cm^{-1} maximum. The relative intensity measured from the Raman signals at 3220 cm^{-1} versus time is shown in **Figure 9**. This intensity increased in samples stored at −10 and −30 °C

after about 16 and 24 weeks of storage, respectively. No significant differences were found as a function of temperature (**Table 2**).

DISCUSSION

Shear resistance measured by the Kramer cell has been found to correlate with sensory hardness in frozen-stored fish (*35*). The ultrastructural analyses in this work showed clear changes as a function of the time and temperature, in terms of fiber organization, intermyofibrillar spaces, and filament lattice (**Figures 3−5**). This is consistent with findings for cod muscle as regards fiber organization and intermyofibrillar spaces (*4*), and with findings of other authors as regards the compaction of the filament lattice (*10*). A question arises as to how these ultrastructural changes are related to the differences in shear resistance found as a function of time and temperature. On one hand, the most important ultrastructure differences between temperatures were found in the changes occurring at the intermyofibrillar spaces. As depicted in **Figure 4**, no reduction of the intermyofibrillar space at −30 °C was observed; however, the intermyofibrillar space decreased progressively at −10 °C, eventually causing the myofibrils to pack together as if "cemented". No big differences in interfiber distances were observed in samples stored at −10 and −30 °C for 38 weeks (**Figure 3D,3E**). The results nevertheless showed a significant increase of shear resistance at −10 °C. The other ultrastructural changes observed at −10 °C, such as fusions between thick filaments (**Figure 5C,D**), do not seem to relate closely to shear resistance, since they were also apparent to some extent at −30 °C after 38 weeks (**Figure 5E,F**). Studies performed on cod have shown that myofibrils pack together during frozen storage and produce a stiffer, firmer fiber and hence a tougher product (*4*). It has been proposed that the sarcoplasmic reticulum degradation occurring during frozen storage may act as a cement holding fibrils together and could contribute significantly to the textural change in frozen-stored fish (*4, 7*). We have confirmed these results for hake muscle.

It has long been assumed that changes in hardness and functional properties such as apparent viscosity, extractability, or water holding capacity of fish muscle are related to protein denaturation and/or aggregation. The apparent viscosity and extractability of fish muscle proteins do undergo changes (*2, 36, 37*) which have trends similar to those of the changes in shear resistance found in the present work. However, changes in these functional properties and in texture do not always parallel structural changes as measured by Raman spectroscopy (*1, 2*) or differential scanning calorimetry (*37−39*). It has been suggested that the joining of myofibrils will reduce the amount of protein obtainable by extraction with salt solutions (*8, 40*). We may therefore assume that the cementation of myofibrils shown in this study could play a significant role in the loss of functional properties such as extractability and apparent viscosity. Both require prior extraction of actomyosin in NaCl solutions at high ionic strength (*41*). It therefore seems reasonable to assume that the aggregation observed during extraction in NaCl solutions is to a large extent due to the "cementing" of myofibrils, paralleling the observed evolution in texture. Further research is needed to determine the extent to which secondary and tertiary structural changes "modulate" loss of these functional properties in this species.

Nevertheless, there are other functional properties, such as WHC, which do not depend on the extractability of muscle proteins. This is a very important parameter, which has been reported to correlate well with sensory attributes such as

juiciness of fish muscle (*42*). Changes in WHC have been partially attributed to the formation, growth, and distribution of ice crystals (*43*). This is consistent with results depicted in **Figure 3** in which these phemomena occur gradually with time, being more pronounced at the higher temperature. However, the cementing of myofibrils does not run in parallel with the changes observed in WHC in these experimental conditions. **Figure 2** shows a gradual decrease of this functional property for both temperatures, whereas ultrastructural results at the intermyofibrillar level display a completely different pattern for both storage temperatures.

WHC changes have been explained in terms of alterations in protein−water interactions (*44, 45*). We have demonstrated through Raman spectroscopy that frozen storage of fish muscle proteins involves secondary structural changes and increased exposure of hydrophobic aliphatic side chains (*1, 2*), which can be related to changes in protein−water interactions. This is reflected more directly by the spectral changes in the Raman band centered at 160 cm^{-1} during frozen storage (**Figure 7**).

On the other hand, there are reports of a strong correlation between low-field NMR relaxation times in meat samples and the WHC of the meat (*46−48*). NMR relaxation times provide information about the compartmentalization and mobility of water in meat (*49−52*). It has also been shown that NMR relaxation times can reveal the number of distinct water pools and the relative pool size in frozen minced cod, although the causal relationship between changes in water distribution and loss of quality still remains to be established (*13*). A detailed knowledge of the water pools in terms of physical location and mobility is therefore necessary. In this connection, the Raman spectral region between 3100 and 3500 cm^{-1} has been reported to reflect the structural changes of water, which are related to the size and mobility of the water pools. Lafleur et al. (*16*) have demonstrated that there is an increase in the intensity of the ν_s(OH) water band in the transition from small water interstices, of the same magnitude as muscle filament spacing ($\sim$1.7 nm), to greater domains of water ($\sim$15 nm). It has been shown that the origin of this spectral change in ν_s(OH) intensity is not dependent on the nature of the surface water biosystem but is dependent on the presence of an autoassociated supramolecular water structure which generates intermolecular vibrational coupling. It therefore seems reasonable to attribute the ν_s(OH) spectral changes in **Figure 9** to transfer of interstitial water to increasing intra- or extracellular spatial domains of 15 nm or larger. This is consistent with the increase in fusions of the filament lattice with storage time that occurs to some extent at both temperatures (**Figure 5**). It can be inferred from Lafleur's theory (*16*) that both intermyofibrillar and extracellular water may be considered as bulk water in the Raman spectra; this could explain the lack of significant temperature-mediated differences (**Figure 9**) as compared with the obvious differences in ultrastructure at the level of fiber organization and intermyofibrillar organization (**Figures 3** and **4**). The lack of significant differences could also be partly due to the large standard deviations found for some of the samples.

Raman spectroscopy shows shifts in both water−protein interactions and water mobility to larger spatial domains. Despite the fact that these phenomena are known to be related to WHC, the evolution of WHC is not coincident in time with either the 160 cm^{-1} or ν_s(OH) band (**Figures 2**, **7**, and **9**). Besides the above considerations, the difference in behavior may be partially attributable to the measurement processes: during WHC measurements, water mobility in the samples is affected by centrifugal force, whereas it is unchanged by spectral measure-

Structural Changes in Hake Muscle during Frozen Storage

J. Agric. Food Chem., Vol. 53, No. 7, 2005   **2565**

ments. This result calls for further research to clarify the potential relationship between changes in water structure and mobility and alterations in WHC.

Conclusion. Increasing muscle hardness and loss of WHC during frozen storage is accompanied by aggregation of fish muscle at two different levels: (a) cementation of myofibrils and (b) increased fusion of myofilaments. It is also accompanied by changes in water−protein interactions and the mobility of water to larger domains. In view of the time/temperature differences among changes in structure, ultrastructure, and functionality, it seems likely that cementation of the myofibrils is the main cause of increased muscle hardness and it is indirectly responsible for loss of functional properties where the first step in the process is extraction of myofibrillar proteins. WHC seems to relate more to protein aggregation at the myofilament lattice level than to cementation of myofibrils.

LITERATURE CITED

(1) Careche, M.; Herrero, A. M.; Rodriguez-Casado, A.; Del Mazo, M. L.; Carmona, P. Structural changes of hake (*Merluccius merluccius* L.) fillets: Effects of freezing and frozen storage. *J. Agric. Food Chem.* **1999**, *47*, 952−959.

(2) Herrero, A. M.; Carmona, P.; Careche, M. Raman spectroscopic study of structural changes in hake (*Merluccius merluccius* L.) muscle proteins during frozen storage. *J. Agric. Food. Chem.* **2004**, *52*, 2147−2153.

(3) Love, R. M. Freezing of animal tissue. In *Cryobiology*; Meryman, H. T., Ed.; Academic Press: New York, 1966; pp 317−406.

(4) Howgate, P. Fish. In *Food Microscopy*; Vaughan, J. G., Ed.; Academic Press Inc.: London, U.K., 1979; pp 343−392.

(5) Shenouda, S. Y. K. Theories of protein denaturation during frozen storage of fish flesh. *Adv. Food Res.* **1980**, *26*, 275−311.

(6) Bello, R. A.; Luft, J. H.; Pigott, G. M. Ultrastructural study of skeletal fish muscle after freezing at different rates. *J. Food Sci.* **1982**, *47*, 1389−1394.

(7) Connell, J. J. Changes in amount of myosin extractable from cod flesh during storage at-14 °C. *J Sci. Food Agric.* **1962**, *13*, 607−617.

(8) Jarenback, L.; Liljemark, A. Ultrastructural changes during frozen storage of cod (*Gadus morhua* L.). *J. Food Technol.* **1975**, *10*, 229−325.

(9) Tanaka, K. Electron-microscopic studies on toughness in frozen fish. In *The Technology of Fish Utilization*; Kreuzer, R., Ed.; Fishing News Books: London, U.K., 1965; pp 121−125.

(10) García, M. L.; Martín-Benito, J.; Solas, M. T.; Fernández, B. Ultrastructure of the myofibrillar component in cod (*Gadus morhua* L.) and hake (*Merluccius merluccius* L.) stored at −20 °C as a function of time. *J. Agric. Food Chem.* **1999**, *47*, 3809−3815.

(11) Lambelet, P.; Renevey, F.; Kaaki, C.; Raemy, A. Low-field nuclear magnetic resonance relaxation study of stored processed cod. *J. Agric. Food Chem.* **1995**, *43*, 1462−1466.

(12) Jepsen, S. M.; Pedersen, H. T.; Engelsen, S. B. Applications of chemometrics to low-field 1H NMR relaxation data of intact fish flesh. *J. Sci. Food Agric.* **1999**, *79*, 1793−1802.

(13) Jensen K. N.; Guldager, H. S.; Jørgensen, B. M. Three-way modelling of NMR relaxation profiles from thawed cod muscle. *J. Aquat. Food Prod. Technol.* **2002**, *11*, 201−214.

(14) Cavatorta, F.; Fontana, M. P.; Vecli, A. Raman spectroscopy of protein-water interactions in aqueous solutions. *J. Chem. Phys.* **1976**, *65*, 3636−3640.

(15) Walrafen, G. E.; Fisher, M. R. Low-frequency Raman scattering from water and aqueous solutions: a direct measure of hydrogen bonding. *Methods Enzymol.* **1986**, *127*, 91−105.

(16) Lafleur, M.; Pigeon, M.; Pézolet, M.; Caillé, J. P. Raman spectrum of interstitial water in biological systems. *J. Phys. Chem.* **1989**, *93*, 1522−1526.

(17) Maeda, Y.; Kitano, H. The structure of water in polymer systems as revealed by Raman spectroscopy. *Spectrochim. Acta* **1995**, *51*, 2433−2446.

(18) Gniadecka, M.; Nielsen, O. F.; Christensen, D. H.; Wulf, H. C. Structure of water, proteins and lipids in intact human skin, hair and nail. *J. Invest. Dermatol.* **1998**, *110*, 393−398.

(19) Gniadecka, M.; Nielsen, O. F.; Wessel, S.; Heidenheim, M.; Christensen, D. H.; Wulf, H. C. Water and protein structure in photoaged and chronically aged skin. *J. Invest. Dermatol.* **1998**, *110*, 1129−1133.

(20) Colaianni, S. E. M.; Nielsen, O. F. Low-frequency Raman spectroscopy. *J. Mol. Struct.* **1995**, *347*, 267−284.

(21) Roussel, H.; Cheftel, J. C. Characteristics of surimi and kamaboko from sardines. *Int. J. Food Sci. Technol.* **1988**, *23*, 607−623.

(22) Roussell, H.; Cheftel, J. C. Mechanisms of gelation of sardine proteins: influence of thermal processing and of various additives on the texture and protein solubility of kamaboko gels. *Int. J. Food Sci. Technol.* **1990**, *25*, 260−280.

(23) Kramer, A.; Burkardt, G. J.; Rogers, H. P. The shear press. A device for measuring food quality. *Canner* **1951**, *112*, 34−40.

(24) Barroso, M.; Careche, M.; Barrios, L.; Borderías, A. J. Frozen hake fillets quality as related to texture and viscosity by mechanical methods. *J. Food Sci.* **1998**, *63*, 793−796.

(25) Nielsen, O. F. The structure of liquid water. A low-frequency (10−400 cm^{-1}) Raman study. *Chem. Phys. Lett.* **1979**, *60*, 515−517.

(26) Nielsen, O. F. Low-frequency spectroscopic studies of interactions in liquid. *Annu. Rep. Prog. Chem., Sect. C: Phys. Chem.* **1993**, *90*, 3−44.

(27) Terpstra, P.; Combes, D.; Zwick, A. Effect of salts on dynamics of water: A Raman spectroscopy study. *J. Chem. Phys.* **1990**, *92*, 65−70.

(28) Starzak, M.; Mathlouthi, M. Cluster composition of liquid water derived from laser-Raman spectra and molecular simulation data. *Food Chem.* **2003**, *82*, 3−22.

(29) Barret, T. W.; Peticolas, W. L.; Robson, R. C. Laser-Raman light-scattering observations of conformational changes in myosin induced by inorganic salts. *Biophys. J.* **1978**, *23*, 349−358.

(30) Caillé, J. P.; Pigeon-Gosselin, M.; Pézolet, M. Laser Raman study of internally perfused muscle fibers. Effects of Mg^{2+}, ATP and Ca^{2+}. *Biochim. Biophys. Acta* **1983**, *758*, 121−127.

(31) Li-Chan, E. Y. C.; Nakai, S. Raman spectroscopic study of thermally and/or dithiothreitol induced gelation of lysozyme. *J. Agric. Food Chem.* **1991**, *39*, 1238−1245.

(32) Ogawa, M.; Nakamura, S.; Horimoto, Y.; Haejung, A.; Tsuchiya, T.; Nakai, S. Raman spectroscopic study of changes in fish actomyosin during setting. *J. Agric. Food Chem.* **1999**, *47*, 3309−3318.

(33) Liljemark, A. Influence of freezing and cold storage on the submicroscopical structure of fish muscle. In *Freezing and Irradiation of fish*; Kreuzer, R., Ed.; Fishing News Books Ltd.: London, U.K., 1969; pp 140−146.

(34) Walrafen, G. E. 1972. Raman and infrared spectral investigation of water structure. In *Water, A Comprehensive Treatise, Vol1. Physics and Physical Chemistry of Water*; Franks, F., Ed.; Plenum Press: New York, 1972; pp 151−214.

(35) Barroso, M.; Careche, M.; Borderias, A. J. Quality control of frozen fish using rheological techniques. *Trends Food Sci. Technol.* **1998**, *9*, 223−229.

(36) Del Mazo, M. L.; Torrejón, P.; Careche, M.; Tejada, M. Characteristics of the salt soluble fraction of hake (*Merluccius merluccius* L.) fillets stored at −20 °C and −30 °C. *J. Agric. Food Chem.* **1999**, *47*, 1372−1377.

(37) Careche, M.; Del Mazo, M. L.; Fernández-Martín, F. Extractability and thermal stability of hake (*Merluccius merlucccius* L.) fillets frozen stored at −10 and −30 °C. *J. Sci. Food Agric.* **2002**, *82*, 1791−1799.

(38) Rodger, G. W.; Weddle, R. B.; Craig, P. Effect of time, temperature, raw material type, processing and use of cryoprotective agents on mince quality. In *Advances in Fish Science and Technology*; Connell, J. J., Ed.; Fishing News Books Ltd.: Surrey, U.K., 1980; pp 199−217.

(39) Davis, J. R.; Ledward, D. A.; Bardsley, R. G.; Poulter, R. G. Species dependence of fish myosin to heat and frozen storage. *Int. J. Food Sci. Technol.* **1994**, *29*, 287−301.

(40) Anderson, M.; Ravesi, E. On the nature of altered protein in cod muscle. *J. Food Sci.* **1970**, *35*, 199−206.

(41) Pomeranz, Y. Proteins: specific foods. In *Functional properties of food components*; Taylor S. L., Ed.; Academic Press: San Diego, 1991; pp 193−247.

(42) Jensen, H. S.; Jorgensen, B. M. A sensometric approach to cod-quality measurement. *Food Qual. Pref.* **1997**, *8*, 403−407.

(43) Bevilacqua, A., N. E. Zaritzky, and A. Cavelo. 1979. Histological measurements of ice in frozen beef. *J. Food Technol. 14*, 237−251.

(44) Offer, G.; Trinick, J. A unifying hypothesis for the mechanism of changes in the water-holding capacity of meat. *J. Sci. Food Agric.* **1983**, *34*, 1018−1019.

(45) Offer, G.; Knight, P. The structural basis of water-holding in meat. In *Developments in Meat Science-4*; Lawrie, R., Ed.; Elsevier Applied Science: New York, 1988; pp 53−173.

(46) BrØndum, J.; Munck, L.; Henckel, P.; Karlsson, A.; Tornberg, E.; Engelsen, S. B. Prediction of water-holding capacity and composition of porcine meat with comparative spectroscopy. *Meat Sci.* **2000**, *55*, 177−185.

(47) Bertram, H. C.; Andersen, H. J.; Karlsson, A. H. Comparative study of low-field NMR relaxation measurements and two traditional methods in the determination of water-holding capacity of pork. *Meat Sci.* **2001**, *57*, 125−132.

(48) Bertram, H. C.; Dønstrup, S.; Karlsson, A. H.; Andersen, H. J. Continuous distribution analysis of T_2 relaxation in meat-an approach in the determination of water-holding capacity. *Meat Sci.* **2002**, *60*, 279−285.

(49) Hazlewood, C. F.; Nichols, B. L.; Chamberlain, N. F. Evidence for the existence or a minimum of two phases of ordered water in skeletal muscle. *Nature* **1969**, *222*, 747−750.

(50) Hazlewood, C. F.; Chang, D. C.; Nichols, B. L.; Woessner, D. E. Nuclear magnetic resonance transverse relaxation times of water protons in skeletal muscle. *Biophys. J.* **1974**, *14*, 583−606.

(51) Bertram, H. C.; Karlsson, A. H.; Rasmussen, M.; Dønstrup, S.; Petersen, O. D.; Andersen, H. J. Origin of multiexponential T2 relaxation in muscle myowater. *J. Agric. Food Chem.* **2001**, *49*, 3092−3100.

(52) Bertram, H. C.; Purslow P. P.; Andersen, H. J. Relationship between meat structure, water mobility, and distribution: A low-field nuclear magnetic resonance study. *J. Agric. Food Chem.* **2002**, *50*, 824−829.